

# Flow Characteristics of a Small-Hole Sieve Tray

Michael W. Biddulph

Derek P. Bultitude

Department of Chemical Engineering

University of Nottingham

Nottingham, United Kingdom

It is now well established that large circular, chordal-weir distillation trays exhibit liquid flow characteristics that are far from the uniform flow usually assumed. The usual tendency for the liquid is to flow preferentially down the center of the tray, leaving slow-moving or stagnant zones around the column walls. It is also now well established that this results in losses of efficiency. Clearly, the more understanding of nonuniform flow phenomena we have the better it is. This is for two reasons. First, this would help predict column efficiencies more accurately, reducing the number of extra trays added to allow for uncertainty. Secondly, and more important, it should lead to better tray designs and to achieving high efficiencies predicted and achieved for uniform flow conditions (Biddulph et al., 1988).

With the aim of understanding more about flow phenomena across large trays, this technique was developed. Previous methods used include dye injection (Bell, 1972), tracer injection (Yu et al., 1982), and temperature variation (Stichlmair, 1987; Porter, 1987). These studies have established a detailed picture of the residence time distribution of fluid elements in the froth. The residence time distribution, however, has its limitations, and a direct, local indication of flow velocity and direction at any point on a tray will be very useful.

## The Technique

The probe as it is mounted into a small air/water simulator for calibration purposes is shown in Figure 1. The probe is independent and movable along a horizontal bar fixed above the test tray parallel to the inlet weir. Using the locking screw, the bottom of the probe is placed just above the tray floor and normal to the direction of froth flow.

Figure 2 shows a schematic view of the probe and its holder. The principle is that the strain created in the probe by the impact of the froth is measured by means of attached strain gauges. The strain-measuring section of the probe consists of: a flat strip of titanium alloy (A), firmly clamped into a holder (B), which was designed to slide into a hollow tube (C) allowing the effective length of the probe to be varied. Near the top of the

titanium alloy strip, a section of the metal (E) is machined to precise specifications. A network of strain gauges is bonded to this area. The gauges are wired together so that between them they form a Wheatstone Bridge network. When there is no froth flow, the bridge is balanced and there is no output voltage. When there is froth flow, the titanium strip bends and the strain gauges deform. The gauges on the side of the probe facing the flow are put under tension, increasing their resistance, while the gauges on the other side are put into compression, decreasing their resistance. The bridge is wired so that this action creates an imbalance; an output voltage, the magnitude of which increases with increasing froth velocity, is produced. Using mathematical theory presented previously by Bultitude (1989) results in the following equation for the output from the probe:

$$V = KV_f^2 h_{CL} C_D \{L - h_F/2\} \quad (1)$$

Flow measuring devices using a similar principle, known as drag plate meters, have been used for some time. They take the form of a circular plate facing the direction of flow and mounted on an arm attached to a null balance. This type, however, is not suitable for installation in the turbulent froth and spray at the center of a large distillation tray. The probe described here has only light electrical connections to the outside of the column. The design details of the probe, including the remote control mechanism for moving it across the tray are available elsewhere (Bultitude, 1989). Table 1 summarizes the dimensions of the probe.

## Calibration of the Probe

Initial trials were carried out in a small purpose-built bench-scale air/water simulator containing a rectangular sieve tray. In this equipment it was possible to achieve liquid weir loadings of up to 35 cm<sup>3</sup>/cm · s and superficial air velocities up to 1 m/s. Promising results were achieved, and good responses to changing weir loading were recorded. To calibrate the probe fully over a wider range of conditions, a modified tray was installed in a

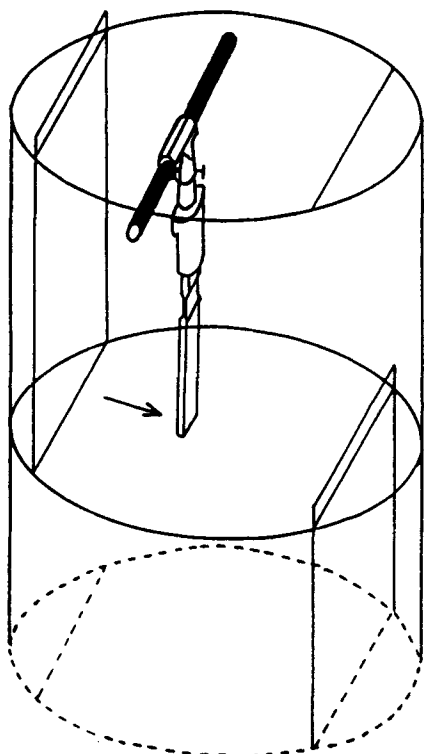


Figure 1. Location of the test probe in the 0.69-m column.

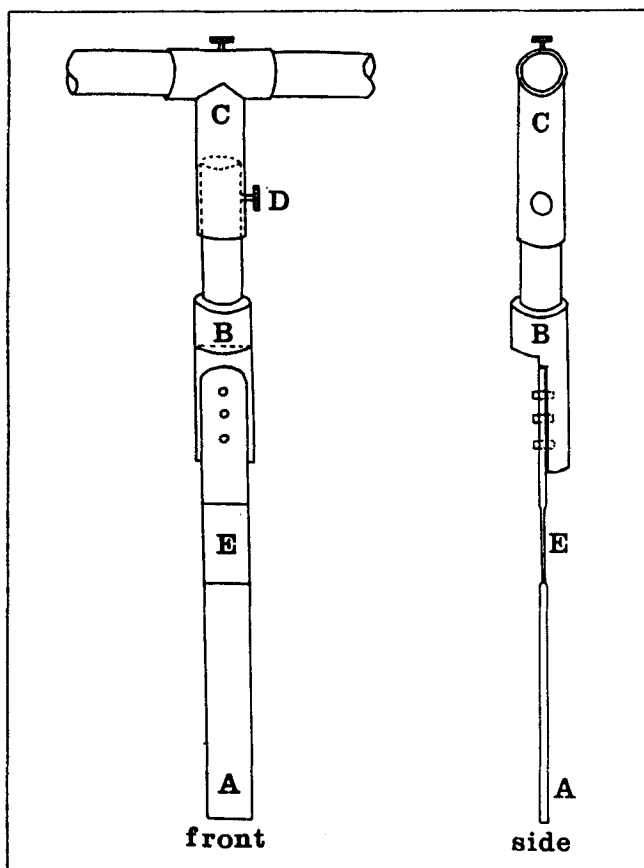


Figure 2. Probe and its holder.

Table 1. Design of the Probe

Width	20 mm
Thickness	1.49 mm
Length	194 mm
Modulus of elasticity	$113.8 \times 10^9 \text{ N} \cdot \text{m}^{-2}$

0.69-m-diameter air/water simulator which was described previously by Biddulph (1975). The tray used was a small-hole sieve tray of the type which is common in the air separation industry. It was modified to provide a rectangular flow channel by blanking off the sides of the tray and attaching aluminium wings. The inlet downcomer was packed with pall rings to ensure a uniform liquid inlet. On this tray, the average froth velocity at a point could be calculated from the weir loading and the clear liquid height. Table 2 shows the main features of this modified tray.

This calibration was carried out with two main goals:

1. To show that the probe could give a sensible output reliably and reproducibly for a given froth velocity
2. To produce a set of calibration curves.

These curves could then be used subsequently when the probes were installed into the 1.8-m-diameter air/water simulator, using sieve tray material of the same type at the same air and water loadings. The probe was tested fully at combinations of various loadings: superficial air velocities of 0.9, 1.0 and 1.2 m/s; weir heights of 0, 0.5 in. (13 mm) and 1 in. (25 mm); and liquid weir loadings from 0–60  $\text{cm}^3/\text{cm} \cdot \text{s}$ . For each set of conditions, the biphasic height was recorded, the clear liquid head was measured using a manometer, and the output signal from the probe was recorded on a pen recorder. Figure 3 shows an example plot. It can be seen that the output increases with weir loading. The phenomenon of lower output at greater weir heights reflects the changes in froth height and clear liquid head, the force acting lower on the probe at low weir heights.

A least squares regression of 137 data points (Bultitude, 1989) results in the following relation:

$$C = \frac{V}{(L - h_F/2)h_{CL}} = 0.243 V_F^{1.2} \quad (2)$$

which, when compared with Eq. 1, indicates a dependence of  $C_D$  on froth velocity.

This dependence turns out to be:

$$C_D = 61.5/[V_F^{0.793}] \quad (3)$$

Figure 4 shows all data points as a calibration curves.

Table 2. Design of Modified Tray

Hole diameter	1.8 mm
Free area	8%
Weir length	480 mm
Tray thickness	2 mm
Hole arrangement	Triangular
Flow path length	489 mm

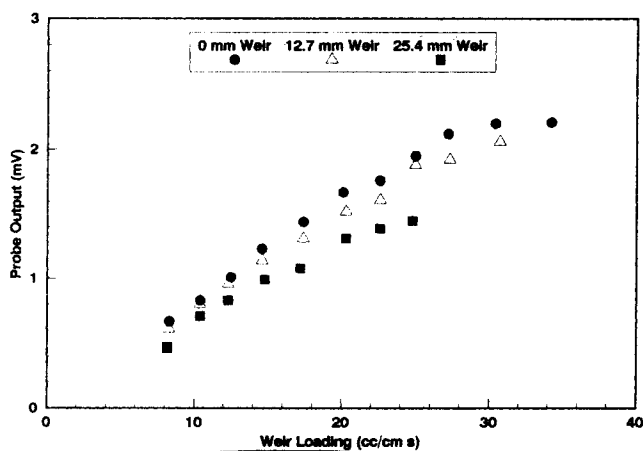


Figure 3. Probe response to water loading.

### Determination of Froth Flow Direction

It has been established that the local direction of froth flow at a point on a tray can be determined by using the probe. This was determined in the following way. The probe was rotated to known angles to the direction of froth flow and the output recorded. The output as a function of angle showed the expected reduction. It was observed that with the angle close to 90 degrees (having the flat face of the probe nearly in line with the froth flow), the change of output with angle is large. Whereas, with the angle close to zero, it is with the probe nearly normal to the flow, the response of output to angle is small. Therefore, the method used to determine the angle of flow direction, was to detect the direction by searching for zero output and then to turn the probe through 90 degrees to measure the velocity. This technique required that the probes installed in the 1.8-m air/water simulator would have to be remotely controlled for rotation and traversing. The method of achieving this was described previously by Bultitude (1989).

### Depth of the Probe in the Biphase

The effect of the position of the bottom of the probe with respect to the tray floor was studied to establish the sensitivity to the clearance above the tray and to measure the response of the probe output to depth into the froth. The results showed that the

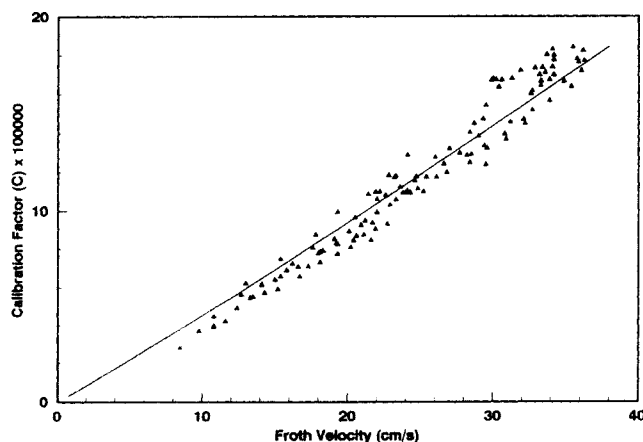


Figure 4. Calibration curve for the probe.

Table 3. Experimental Conditions of 1.8-m Column

Run No.	Air Velocity	Weir Loading	Weir Height	Inlet Downcomer
	m/s	cm <sup>3</sup> /cm · s	mm	
P	0.8	35	25	Unpacked
Q	0.8	35	25	Packed
R	0.8	70	25	Packed
S	0.8	100	25	Packed
T	1.1	70	25	Packed
U	0.8	70	51	Packed
V	0.8	35	51	Packed

output is indeed sensitive to the clearance and that this must be allowed for carefully in large tray studies. The differing output from the probe at different depths can, with certain assumptions, be used to infer a froth density profile (Bultitude, 1989).

### Local Velocities on a Large Tray

A system developed for moving the probes within the large column had the following characteristics:

- Five supporting bars were established, parallel to the weirs and equally spaced from inlet to outlet. Each bar had a probe mounted onto it.
- A probe could be moved in both directions along a bar and locked in position.
- A probe, once locked in position on its bar, could be rotated, locked, and the angle of flow determined.

Measurements were made at 20 cm intervals along the bars.

### Results

Output voltages from all the probes were collected and processed by on-line computer, where tray unevenness, froth

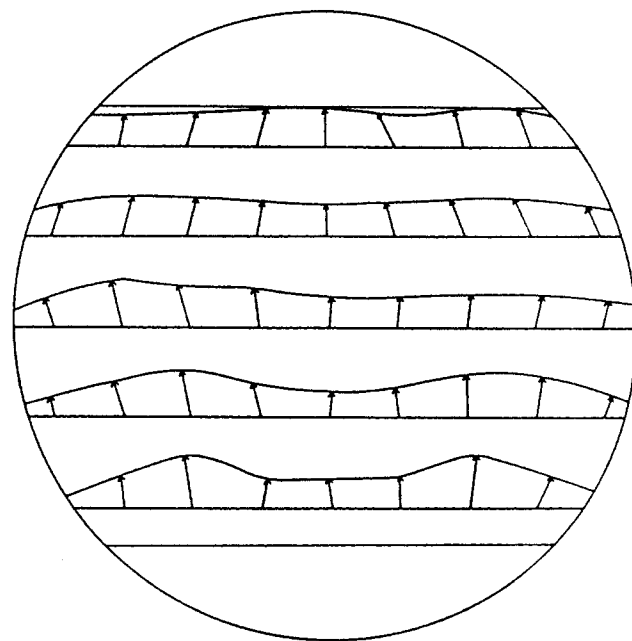
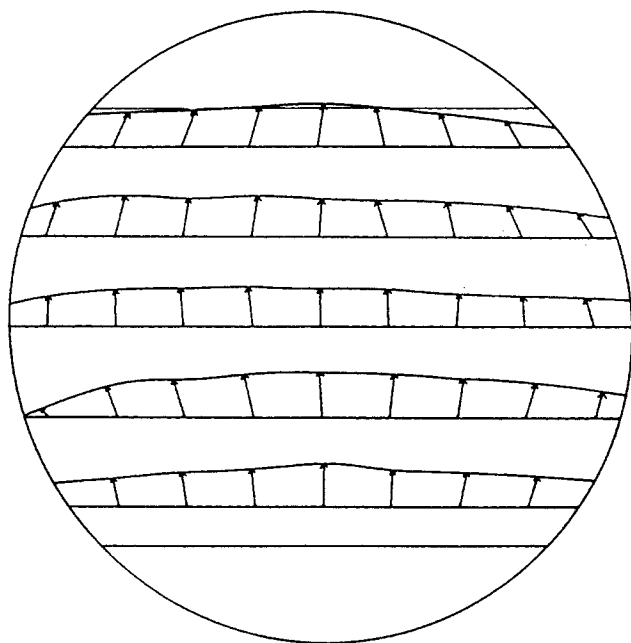


Figure 5. Velocity Distribution on a 1.8 m diameter sieve tray.

Run P:  $u = 0.8$  m/s,  $W = 35$  cm<sup>2</sup>/s,  $h = 25.4$  mm



**Figure 6. Velocity distribution on a 1.8-m-dia. sieve tray.**  
Run Q:  $u = 0.8$  m/s,  $W = 35$  m<sup>2</sup>/s,  $h = 25.4$  mm, packed inlet downcomer

heights, and clear liquid heads were all accounted for (Bultitude, 1989). Multiple manometers were used to measure the clear liquid heads.

Table 3 shows the conditions used in the seven runs reported here. The results of the froth velocity measurements are shown in Figures 5–6 as well as in Figures 7–11 in the Supplementary Material. The arrows show the local direction of flow, and the length of each arrow is approximately proportional to the magnitude of the local velocity. The details of all these runs are available (Bultitude, 1989). Figures 5 and 6 show velocity distributions on the tray for the same loadings and weir height, but with different downcomer conditions. In Figure 5 the downcomer is unpacked, and the liquid distributor introduces the flow onto the tray with a severely nonuniform distribution. This nonuniform flow persists across the tray, almost to the outlet. Low velocities are seen near the walls. In Figure 6, with the downcomer packed, the inlet flow is mainly down the center of the tray, with low flows near the wall particularly at the left side.

Figure 7 in the Supplementary Material shows the effect of doubling the weir loading, in which quite noticeable nonuniform

flow is observed and the velocities around the walls are much lower than down the center. This is further accentuated in Figure 8, at an even higher loading. Figures 7 and 9 show the effect of increasing air rate on liquid flow distribution. A close examination reveals that the profiles are very slightly flatter at the higher air rate, which seems to be reasonable due to greater turbulence. Figures 10 and 11 show runs with a higher outlet weir. Comparison of these with the runs at the same loadings with the lower weir indicate little effect on weir height within this range. This conclusion, however, may not hold for heavier loadings and deeper weirs.

## Notations

- $C$  = calibration factor,  $V/cm^2$
- $C_D$  = drag coefficient
- $h$  = weir height, mm
- $h_{CL}$  = clear liquid head, m
- $h_F$  = froth height, m
- $K$  = probe constant
- $L$  = effective probe length, m
- $u$  = superficial air velocity, m/s
- $v$  = output voltage from probe, V
- $v_f$  = average froth velocity, m/s
- $W$  = weir loading,  $cm^2/s$

## Literature Cited

- Bell, R. L., "Residence and Fluid Mixing on Commercial-Scale Sieve Trays," *AIChE J.*, **18**, 498 (1972).
- Biddulph, M. W., "Oscillating Behavior on Distillation Trays: II," *AIChE J.*, **21**, 41 (1975).
- Biddulph, M. W., and D. P. Bultitude, "A New Technique for Measuring Local Froth Velocities on Distillation Sieve Trays," *AIChE Meeting*, Houston (1989).
- Biddulph, M. W., M. A. Kalbassi, and M. M. Dribika, "Multicomponent Efficiencies in Two Types of Distillation Column," *AIChE J.*, **34**, 618 (1988).
- Bultitude, D. P., "Distillation Tray Studies," PhD Thesis, Univ. of Nottingham, U.K. (1989).
- Porter, K. E., B. Davies, B. A. Enjugu, and C. C. Ani, "Investigating the Effect of the Liquid Flow Pattern on Sieve Tray Performance by Means of the Water Cooling Technique," *ICHE Symp. Ser.*, **A5**, No. 104, 69 (1987).
- Stichlmair, J., and S. Ulbrich, "Liquid Channelling on Trays and Its Effect on Plate Efficiency," *Chem. Eng. Technol.*, **10**, 33 (1987).
- Yu, K. T., J. Huang, and Z. Zhang, "The Residence Time Distributions and Efficiencies of Large Trays," *Proc. Meeting of Chem. Eng. CIESC and AIChE*, Beijing, China, 425 (1982).

*Manuscript received May 22, 1990, and revision received Oct. 15, 1990.*

See NAPS document no. 04824 for 6 pages of supplementary material. Order from NAPS c/o Microfiche Publications, P.O. Box 3513, Grand Central Station, New York, NY 10163. Remit in advance in U.S. funds only \$7.75 for photocopies or \$4.00 for microfiche. Outside the U.S. and Canada, add postage of \$4.50 for the first 20 pages and \$1.00 for each of 10 pages of material thereafter, \$1.50 for microfiche postage.